Sharp, J.S., Forrest, J.A. & Jones, R.A. Surface denaturation and amyloid fibril formation of insulin at model lipid–water interfaces. Biochemistry 41, 15810–15819

ARTICLE *in* BIOCHEMISTRY · JANUARY 2003

Impact Factor: 3.02 · DOI: 10.1021/bi020525z · Source: PubMed

3 AUTHORS:

James S Sharp
University of Nottingham
55 PUBLICATIONS **914** CITATIONS
SEE PROFILE

James A Forrest
University of Waterloo
122 PUBLICATIONS **4,521** CITATIONS
SEE PROFILE

Lyndon W Jones
University of Waterloo
318 PUBLICATIONS **4,263** CITATIONS
SEE PROFILE

Surface Denaturation and Amyloid Fibril Formation of Insulin at Model Lipid−Water Interfaces

J. S. Sharp,*,‡ J. A. Forrest,‡ and R. A. L. Jones§

Department of Physics, University of Waterloo, 200 University Avenue West, Waterloo, Ontario, Canada N2L 3G1, and Department of Physics and Astronomy, University of Sheffield, Hounsfield Road, Sheffield S3 7RH, England

Received August 8, 2002

ABSTRACT: We consider the effects that different lipid surfaces have upon the denaturation and subsequent formation of amyloid fibrils of bovine insulin. The adsorption and unfolding kinetics of insulin being adsorbed onto the different lipid surfaces under denaturing conditions are studied using FTIR ATR spectroscopy and are compared to the bulk solution behavior of the protein. Atomic force microscopy studies are also performed to compare the fibrils growing on the different surfaces. This study shows that both the adsorption and unfolding kinetics of insulin can be described by a sum of exponential processes and that different surfaces behave differently, with respect both to one another and to the bulk protein solution. The proteins adsorbed onto the surfaces are observed to have faster unfolding kinetics than those in the bulk, and the fibril-like structures formed at the surfaces are shown to be different in a number of ways from those found in bulk solution. The β-sheet content and growth kinetics of the adsorbed proteins also differ from those of the bulk system. An attempt is made to describe the observed behavior in terms of simple physical arguments involving adsorption, unfolding, and aggregation of the proteins.

Protein denaturation and amyloid fibril formation are the key processes that control the onset and development of so-called protein folding diseases such as Alzheimer's disease, systemic amyloidosis, and transmissible spongiform encephalopathy (*1*−*3*). The misfolding of the proteins involved in these diseases leads to the formation of "fibrillation-competent" partially folded intermediates that associate with one another to form fibrils. The onset of fibril formation can be triggered in vitro by exposing proteins to weakly denaturing conditions. This can be achieved by changing parameters such as the temperature, concentration, pH, and ionic strength of the protein solutions.

One of the key differences between conditions in vitro and conditions in vivo is the presence in the latter case of a large amount of interface, in the form of lipid membranes. It is noteworthy that amyloid isolated from patients has a high lipid content. This makes it worth posing the question of how the formation of amyloid fibrils might be affected by the proximity of surfaces and interfaces. There are already indications from experiment that amyloid fibril formation in insulin is strongly promoted at hydrophobic interfaces (*4*). Such an effect might be expected for proteins adsorbed at interfaces in general. It is well-known that adsorption at interfaces can lead to a lowering of the temperature at which proteins denature and form intermolecular associations; this effect depends on both the physical and chemical character of the interface (*5*, *6*).

Detailed studies of the qualitative and quantitative differences between the unfolding and association behavior of proteins when adsorbed at a surface and in bulk have been carried out by Ball et al. (*5*) and Adams et al. (*6*). These experiments demonstrated that the unfolding kinetics of lysozyme at lipid surfaces are faster than those observed in bulk solution. They also showed that aggregation of the protein occurs at temperatures lower than those required in the bulk system. This is manifested as a reduction in the gelation temperature of the protein from 70 to ∼55 °C. This work used FTIR spectroscopy to study structure at the local level, and did not study the morphological character of the aggregates. On the other hand, the work by Sluzky et al. (*4*) used UV absorption spectroscopy and quasi-elastic light scattering to look at the development of the structures of insulin aggregates, the rates of aggregation, and the size of the aggregates formed in the presence of hydrophobic surfaces. It clearly shows that the aggregates formed in the presence of polytetrafluoroethylene (PTFE) surfaces were found to be larger than those found in the solutions without any surfaces. The work by Sluzky et al. also shows that by increasing the surface area of the chemically inert PTFE in contact with the solution, one can increase the rate of aggregation. These studies provide strong evidence that surfaces are important in controlling both the rates and extent of unfolding and aggregation in protein solutions. What is now required are experiments which combine a quantitative study of the way in which surfaces modify the kinetics of unfolding and intermolecular association with microscopic observations of the morphological character of the resulting aggregates.

Protein aggregation often occurs as a result of the formation of β-sheet structures in which the polypeptide backbones from more than one protein molecule are associated. Amyloid fibril formation is a special case of aggregation

* To whom correspondence should be addressed. E-mail: jssharp@sciborg.uwaterloo.ca.

‡ University of Waterloo.

§ University of Sheffield.

10.1021/bi020525z CCC: $22.00
Published on Web 12/03/2002

in which extensive intermolecular β-sheet interactions (*7*) result in the "rope-like" structures observed in amyloid plaques (*8*). The polypeptide chains that make up the β-sheet sections in insulin fibrils have been determined to lie with the chain backbone perpendicular to the fibril growth axis to form a so-called cross-β structure (*9*). The aggregates that form in heat-set gels are also characterized by extensive intermolecular β-sheet interactions (*10*). However, although these aggregates are often characterized by a high β-sheet content, comparable with that found in amyloid fibrils, their external aggregate morphology is much less well defined. It is not at all clear whether this difference in morphology reflects a fundamental difference in the thermodynamics underlying the transition from the native state to the aggregated structures, or whether it is a function of the kinetics of this transition.

Nielson et al. (*11*) have proposed a model for the formation of amyloid fibrils of insulin that starts with hexamer−trimer−dimer units of the protein in solution. The level of association of the protein units is determined by factors such as the concentration, pH, and temperature of the solution. To form fibrils, these hexamer−trimer−dimer units have to first disassociate to form the monomeric protein. The monomeric protein units then need to partially unfold to form the intermediate required to produce the nucleus from which amyloid fibrils can grow.

In this work, we confine protein molecules at an interface and look at how adsorption of the protein affects subsequent aggregate and amyloid fibril formation. We use FTIR ATR spectroscopy to look at the adsorption, unfolding, and β-sheet formation kinetics of the model protein, bovine insulin, under denaturing conditions (acidic pH and elevated temperature). This is done for two different model lipid−water interfaces. The results of these experiments are then compared to bulk FTIR solution data. The spectroscopic measurements are complemented by a series of AFM experiments on the protein-covered substrates in an effort to study the morphology of the aggregates that are formed. This allows us both to distinguish between the formation of amyloid fibrils and less well structured aggregates and to identify differences in the details of the morphology of the fibrils.

Under the conditions chosen for the experiment (pH 1.6 and 60 °C), insulin is dimeric and each insulin molecule carries a charge of +6 (*11*). It is therefore possible to control the interaction between the protein and the surface using the electrostatic interaction between the protein and certain phospholipids with charged headgroups.

The lipids chosen for this study are 1,2-dioleoyl-3-trimethylammonium propane (DOTAP, cationic headgroup) and 1,2-dioleoyl-*sn*-glycero-3-[phospho-*rac*-(1-glycerol)] (DOPG, anionic headgroup). DOTAP experiences a repulsive electrostatic interaction with respect to the insulin molecules, while DOPG experiences an attractive electrostatic interaction with the protein molecules. To ensure that the headgroups of the lipids are at the surface, the lipids are first deposited on to a spin cast polystyrene film from aqueous solution. This ensures that the hydrophobic tail groups associate with the hydrophobic film, leaving the hydrophilic charged headgroups in contact with the aqueous medium. The lipid surfaces chosen for this work are the same as those used in the studies by Adams et al. (*6*) and Sharp (*12*) and are intended to provide a simplistic model of a cellular or biological surface.

EXPERIMENTAL PROCEDURES

Lipid Surface Preparation. The lipids used in this study were obtained from Avanti Polar lipids and were supplied in 100 mg ampules as a white powder. Stock solutions of the lipids were made by dissolving them in chloroform up to a concentration of 10 mg/mL. A pipet was then used to transfer 1 mL of this solution to a volumetric flask, where the chloroform was removed by passing a stream of dry nitrogen through the flask for 1 h. When the chloroform had evaporated, suspensions were made by adding an aqueous solvent to the dried lipid. These were made up to a concentration of 0.1 mg/mL.

In the case of the lipid with the cationic headgroup, 1,2-dioleoyl-3-trimethylammonium propane (MW = 698.55), the aqueous solvent that was used was deionized water (Milli-Q). The solvent used for the lipid with the anionic headgroup, 1,2-dioleoyl-*sn*-glycero-3-[phospho-*rac*-(1-glycerol)] (MW = 797.04), was 0.1 M sodium phosphate buffer (Na_2HPO_4 and NaH_2PO_4) adjusted to pH 7.

The resulting lipid suspensions were then ultrasonicated in an ice−water bath for 30 min. This produced clear solutions, suggesting that the lipid vesicles that were produced were typically smaller than optical wavelengths.

To ensure that the lipids were deposited with their headgroups at the surface, a hydrophobic polystyrene layer was first deposited on the chosen substrate (*6*, *12*). This was done by making 2 wt % solutions of 150 K polystyrene (obtained from Polymer Source) by dissolving the polymer in toluene. The solutions were then spin-coated at 3000 rpm on to the chosen substrate. The thickness of the resulting films was determined using ellipsometry, and the films produced by this method were typically 86 nm thick. The rms roughness of the polystyrene layer was typically found to be 0.2 nm (as measured using AFM). To remove any excess solvent in the films and to relax any stresses introduced by the spin coating process, the films were annealed under vacuum at 120 °C for 30 min.

The lipids were deposited on to the polystyrene films by immersing the PS-coated substrates in the lipid suspensions for 20 min at room temperature. Previous work (*12*) has shown that this procedure results in a uniform layer of lipid, consistent with the deposition a single monolayer of material. This was confirmed by using a quartz crystal microbalance (QCM) to measure the mass of adsorbed lipid deposited on a polystyrene-coated quartz crystal. In both cases, a mass change consistent with the deposition of a single monolayer of lipid was observed.

To determine the stability of these lipid layers in the presence of the denaturing medium to be used in the protein experiments [0.025 M HCl and 0.1 M NaCl (pH 1.6) at 60 °C], the QCM was used to monitor mass changes in the lipid layer as this solution was passed over the surface of the sample. No significant changes were observed in the mass of the lipid layer over a period of 3 h, even when the sample and solution were heated to 60 °C.

Protein Solution Preparation. The protein solutions used for the FTIR measurements were prepared by making a solution of 0.025 M HCl and 0.1 M NaCl in D_2O. Bovine

insulin (Sigma Aldrich, Mw = 5733) was dissolved in this denaturing medium and made up to a concentration of 10 mg/mL. The solutions were left for 24 h at room temperature to ensure that all the labile hydrogens were exchanged with deuterium.

The solutions used for the AFM experiments described below were prepared in exactly the same way except that H_2O was used instead of D_2O.

Fourier Transform Infrared Attenuated Total Reflection (FTIR ATR) Spectroscopy. The FTIR spectrometer used in these studies was a Bio-Rad Excalibur model. The squarecol heated liquid cell used in this work was obtained from Graseby-Specac and uses a parralelopiped-shaped ZnSe crystal as the substrate. In the ATR geometry, infrared radiation is totally internally reflected off the interface between the ZnSe crystal and the system of interest (in our case a lipid-covered PS layer). This produces an exponentially decaying evanescent wave that typically penetrates 1 μm into the sample. Any absorbing species that approaches or adsorbs to the sample surface will remove energy from the evanescent field and give rise to an absorption spectrum. The exponential spatial dependence of this field and its short penetration depth mean that the technique is sensitive only to a small volume of material just above the surface of the ZnSe crystal.

The polystyrene layer was deposited onto both sides of the ATR crsytals by spin coating the polymer solution. The films were then annealed at 120 °C under vacuum, slowly cooled to room temperature, and placed in the liquid cell. Lipid solutions were then introduced into the cell and allowed to adsorb at room temperature for 20 min. The cell was then flushed with a solution of the denaturing medium (0.025 M HCl and 0.1 M NaCl in D_2O), heated to 60 °C, and allowed to equilibrate. A background spectrum was collected using a resolution of 4 cm^{-1}, and an average of 250 scans were taken per spectrum.

The denaturing medium was then exchanged for a solution consisting of 10 mg/mL bovine insulin dissolved in the denaturing medium. The cell volume was exchanged many times with the protein solution to ensure that the protein concentration remained at 10 mg/mL. Thermal equilibration of the protein solution with the ATR cell typically took 1−2 min. Spectra were taken using a resolution of 4 cm^{-1}, initially at intervals of 10 min for a period of 2 h and then every 30 min for a further 22 h. In each case, 50 scans were averaged per spectrum.

Bulk solution studies were also performed using a FTIR liquid transmission cell with a path length of 12 μm (Graseby-Specac). The denaturing medium was injected into the cell, the cell heated to 60 °C, and a background spectrum collected (resolution of 4 cm^{-1}, 250 scans averaged per spectrum). The transmission cell volume was then exchanged for an excess of 10 mg/mL bovine insulin in the denaturing medium. Equilibration of this solution with the cell was determined to take less than 1 min. Spectra were collected every 10 min for 2 h and then every 30 min for a further 22 h.

Atomic Force Microscopy. Atomic force microscopy measurements were performed on the sample surfaces using a Thermo Microscopes Explorer atomic force microscope in noncontact mode.

The lipid surfaces used were prepared as described above on 1 cm × 1 cm single-crystal silicon wafers (⟨100⟩ crystal plane, Compart technology).

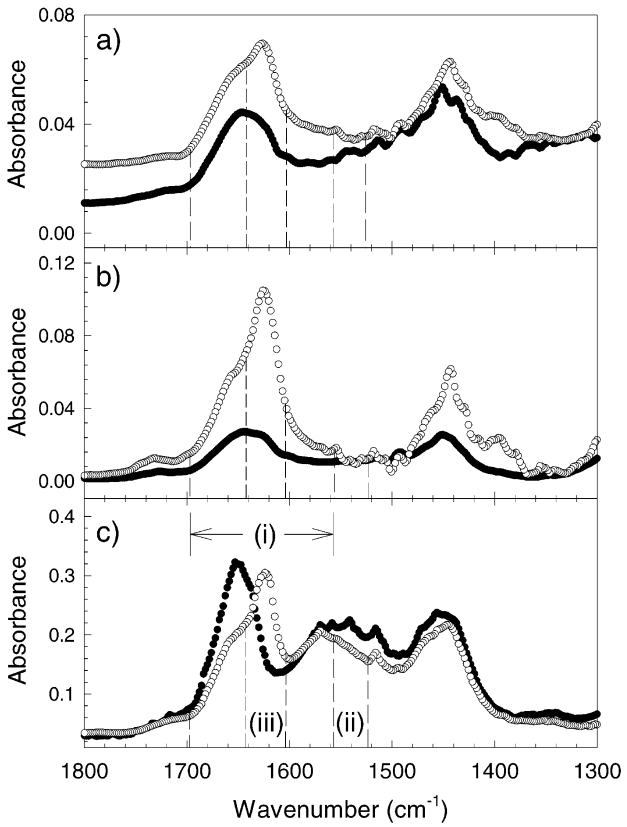

FIGURE 1: Spectra of 10 mg/mL bovine insulin in denaturing medium (0.025 M HCl and 0.1 M NaCl) at 60 °C for the protein (a) adsorbed at the electrostatically repulsive DOTAP surface, (b) adsorbed at the electrostatically attractive DOPG surface, and (c) in bulk solution. Data are shown for spectra collected at time t = 0 (●) and after 2 h in denaturing medium (○). The dashed lines mark the boundaries of the regions used to determine (i) the amide I peak area, (ii) the amide II peak area, and (iii) the β-sheet content of the protein.

Lipid-coated polystyrene films, supported on silicon substrates, were then placed in a 10 mg/mL solution of bovine insulin in the denaturing medium (0.025 M HCl and 0.1 M NaCl). The films were suspended facing downward into the solution to eliminate any effects due to sedimentation, and the solutions were heated to 60 °C. At each 10 min interval, a substrate was removed, rinsed with the denaturing medium, dried with nitrogen, and imaged on the atomic force microscope. This was repeated for both lipid surfaces.

Bulk measurements of the fibrils were also carried out by removing an aliquot of the protein solution at each 10 min interval. Each of these samples was then diluted by a factor of 10 using the denaturing medium (0.025 M HCl and 0.1 M NaCl) and a drop placed on a clean silicon substrate and allowed to dry. When this was being done, care was taken care to remove the sample from a region of the solution away from the air−water interface and the sides of the vial. This was done to avoid collection of fibrils that had formed at these interfaces. Once the droplet had dried, the surface was imaged using the atomic force microscope.

RESULTS AND DISCUSSION

Typical FTIR spectra of bovine insulin, taken using both the ATR geometry and the liquid transmission cell, are shown

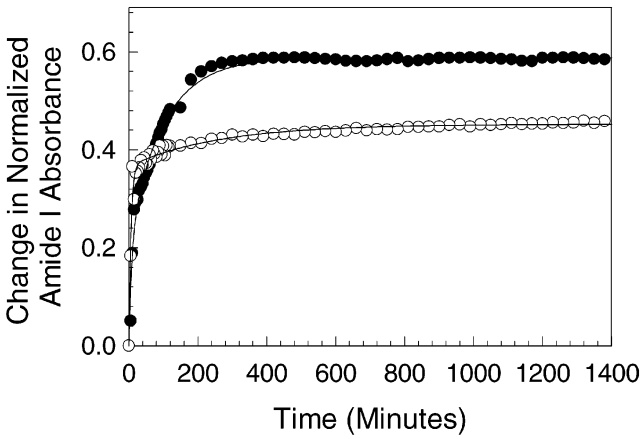

FIGURE 2: Kinetics of the adsorption of insulin on to the two lipid surfaces. Data are shown for adsorption onto the (○) DOTAP and (●) DOPG surfaces. The solid lines are fits to the double-exponential form of eq 1.

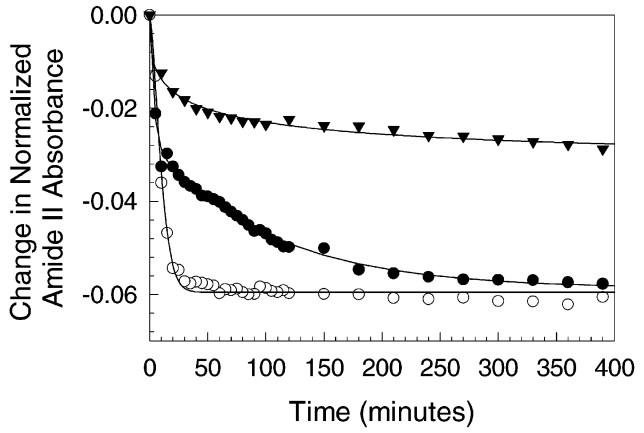

FIGURE 3: Insulin unfolding kinetics. Data are shown for the protein (▼) in bulk solution and adsorbed onto the (○) DOTAP and (●) DOPG surfaces. Solid lines represent the best fits to multiexponential forms.

in Figure 1. The solid symbols give the protein spectra at time $t = 0$, and the open symbols show the same spectra after immersion for 2 h in the denaturing medium. Both were taken at a temperature of 60 °C. Panels a and b of Figure 1 show data collected for the lipid surfaces. They clearly show that as time progresses the total absorbance increases, indicating that an increased amount of protein is deposited at the lipid−water interface. These spectra also change shape as time progresses, indicating that structural changes occur in the protein. The adsorption kinetics of the protein need to be decoupled from these structural changes. This is done by monitoring the integrated absorbance over the whole amide I absorption band (1695−1555 cm^{-1}) which is due to C═O stretching coupled to N−H bending and C−H stretching modes. Figure 2 shows the change in amide I peak area normalized by the total integrated absorbance over the whole amide region (I and II) (1900−1350 cm^{-1}).

Figure 3 shows a plot of the change in the integrated absorbance of the amide II region (1550−1531 cm^{-1}) normalized to the integrated area of the whole amide region. The structural changes that give rise to the decreasing value of the normalized amide II intensity can be attributed to the unfolding of the protein (*5*, *6*). These changes occur because the unfolding protein molecules expose hydrogenated amide

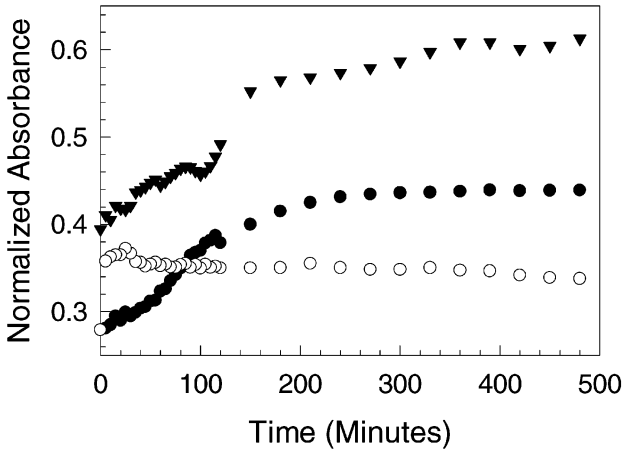

FIGURE 4: β-Sheet formation kinetics in insulin. Data are shown for the protein (▼) in bulk solution and adsorbed onto the (○) DOTAP and (●) DOPG surfaces.

groups in their cores that were not originally exchanged in the D_2O solution. The exchange of these hydrogens for deuterium causes a shift in the vibrational frequency of this absorption band to lower frequencies. Determining the area of this peak as a function of time therefore allows us to monitor the unfolding kinetics of the protein.

Similar information about unfolding was also obtained from the spectra for the bulk solution data. This is also plotted in Figure 3. However, it is worth stressing that no change in the relative absorbance in the amide I region is observed. This arises because no surface adsorption is detected because the amount of material in the beam path remains constant.

The growth of the shoulder at 1635−1604 cm^{-1} has been attributed to increases in the β-sheet content of the protein (*5*, *6*). Figure 4 shows the normalized changes in the absorbance of this shoulder with time for both of the lipid surfaces and for the bulk system.

Kinetics of Protein Adsorption. The data depicted in Figure 2 show that the adsorption of insulin onto the two oppositely charged surfaces occurs, initially, at the same rate. After approximately 10 min, the rate of change of the normalized amide I area changes, resulting in different time constants for the two different surfaces. The discovery of two apparently different processes during adsorption of protein onto these surfaces has been reported recently for lysozyme (*6*, *12*). The adsorption data obtained were fitted to the double-exponential form

$$A = A_1\left[1 - \exp\left(-\frac{t}{t_1}\right)\right] + A_2\left[1 - \exp\left(-\frac{t}{t_2}\right)\right] \quad (1)$$

where A is the absorbance, A_1 and A_2 are constants, and t_1 and t_2 are the corresponding time constants of the two processes.

Fits to the data are shown as solid lines. They show that the time constant for the initial adsorption is between 384 and 492 s for both of the surfaces that were studied. The time constant for the second process was determined to be 6000 ± 360 s for the DOPG surface and 15 780 ± 288 s for the DOTAP surface.

Care has to be taken when extracting adsorption kinetics from FTIR ATR data, because of the structural changes that alter the strength of the dipole moments and result in changes in the shape of the amide I band. These changes can be

misinterpreted as a change in the amount of adsorbed material if the correct method of analysis is not used. The comparative studies performed on lysozyme using FTIR ATR (*6*) and the QCM (*12*) gave similar adsorption kinetics. These studies suggest that the FTIR data obtained from the amide I region (normalized to the area of the amide I and II regions) provide a valid method for determining the amount of material adsorbed at an interface.

A quartz crystal microbalance (Q-Sense) was used to monitor the adsorption of insulin under the conditions used in the FTIR experiments. These experiments confirmed the time scales for adsorption that are given above. This technique uses the change in frequency of a quartz crystal mechanical oscillator to detect changes in the mass of the material adsorbed on the crystal surfaces. The quartz crystal microbalance is capable of detecting submonolayer coverage of large molecules such as polymers and proteins.

These experiments gave equilibrium changes of 69 ± 1 Hz for the DOTAP surface and 94 ± 2 Hz for the DOPG surface. These changes correspond to the deposition of surface excesses of protein equivalent to 12.07 ± 0.01 and 16.45 ± 0.01 mg/m^2, respectively. The expected surface coverage for a monolayer of insulin, calculated using the radius of gyration of the protein in solution [1.16 nm at pH 1.6 (*11*)], is 6.82 mg/m^2. This means that the adsorbed amount of insulin detected in the experiments is consistent with the deposition of between two and three monolayers of protein for both of the surfaces that were studied. This assumes that the insulin is deposited in complete monolayers and represents an average of the amount of protein deposited over the whole surface of the quartz crystal. However, we show below that the aggregation of insulin results in a nonuniform distribution of protein being deposited at both of the surfaces that were studied.

Insulin Unfolding and β-Sheet Formation Kinetics. The amide II peak area was used to determine the stability of the natural globular state of the proteins adsorbed at each of the interfaces and in the bulk solution. The shift in frequency of the band at 1550−1530 cm^{-1} to the band around 1400 cm^{-1} can be attributed to the H−D exchange of previously unexposed NH groups in the protein core (*6*). When the tertiary structure of the protein "loosens", these NH groups become more accessible to the deuterated solvent.

Figure 3 shows the change in the normalized area of the amide II peak for both surfaces studied and for the bulk. This figure shows that unfolding of the insulin molecules occurs much faster on both of the surfaces than it does in the bulk. Unfolding on the repulsive DOTAP surface is the fastest of the three cases that have been studied. This is interpreted as being due to the unfavorable interaction between the DOTAP surface and the insulin molecules that forces the molecules to adopt a more favorable conformation for adsorption (*6*).

Exponential fits were also performed on the unfolding data shown in Figure 3 (solid lines). For the case of the DOTAP surface data, a single exponential with a time constant of 667 ± 33 s could be used to describe the unfolding of the insulin molecules. The data obtained for unfolding at the DOPG surface contain at least two different processes, so the data were fitted to a double-exponential form (eq 1). The shorter time unfolding process was determined to have a time constant of 202 ± 26 s, while the longer time process has a time constant of 6122 ± 360 s. The slower unfolding kinetics observed on the DOPG surface are attributed to the increased stability of the natural globular state of the insulin molecules when adsorbed onto an attractive surface (*6*).

Fits to the bulk unfolding data shown in Figure 3 were also attempted. It was found that these data could not be reliably fit using a single- or double-exponential form. Larger numbers of exponentials could have been used, but this would detract from the simplicity of the arguments used and would yield very little information. The processes that mediate unfolding of the proteins are likely to be highly complex, and to hope to be able to use such a simple model is perhaps unrealistic. It is possible to identify at least two different processes in the bulk data. The short time process has a time constant of around 800 s, and the longer time process has a time constant of 200 000 s.

The unfolding of insulin under the bulk solution conditions used here is much slower than previously described. Studies by Buijs et al. (*13*) have shown that the characteristic unfolding time for insulin at pH 7 and 21 °C is approximately 1700 s. Proteins in general are known to denature more rapidly at elevated temperatures and under acidic conditions (*14*). However, the results presented here are supported by the results of a study by Bryant and co-workers (*15*) which shows that the conformational stability of insulin is actually increased under acidic conditions.

The β-sheet content of the protein can be used as a marker for the level of aggregation in the system (*6*). Figure 4 shows the change in the area of the β-sheet shoulder (1635−1604 cm^{-1}) normalized to the area of the whole amide (I and II) region. This figure shows that the protein in the bulk solution contains a much higher β-sheet content than the protein adsorbed at either of the two surfaces used in this study. The bulk data initially show a steady increase in β-sheet content as the protein denatures and aggregates. After approximately 120 min, an abrupt increase in the β-sheet content is observed. This is consistent with the fact that the bulk solutions that are used form a clear gel around this time, indicating a dramatic increase in the level of aggregation in the solution. After this point, the β-sheet content continues to increase slowly and was still increasing after 24 h.

Both of the surfaces show a reduction in the amount of β-sheet formed per unit volume when compared to the bulk. The protein on the repulsive DOTAP surface shows the smallest extent of β-sheet formation. The kinetics of β-sheet growth are also much faster on both surfaces. The DOTAP surface has the fastest β-sheet growth kinetics and saturates after only 10−15 min in the denaturing medium. The DOPG surface shows a steady initial increase in the β-sheet content with a slope that is similar to that obtained for the bulk data. This again reflects the relative stability of the solution state of the protein when adsorbed at an attractive surface. After 65 min, the rate of β-sheet growth increases until it saturates after 240 min in the denaturing medium. Comparison of the time constants for β-sheet formation with the ones observed for the unfolding of the protein shows they are similar (within a factor of 1.5). This is observed for both of the lipid surfaces and the bulk solution. Aggregation in this system appears to be limited by the unfolding of the proteins.

AFM of Insulin Fibrils and Aggregates. The data shown in Figures 3 and 4 illustrate that protein molecules adsorbed at an interface exhibit behavior significantly different from

the behavior of those in bulk solution. The increased extent of unfolding and reduced β-sheet content observed on the surfaces provide an indication that the structures formed by the protein could be different at the surfaces when compared to those in the bulk. To correlate the structural changes in the FTIR spectra of insulin with actual changes in the morphologies of the observed structures, atomic force microscopy experiments were performed on samples taken from both the bulk solution and each of the surfaces.

In situ imaging of the fibrils proved to be difficult. Under the conditions used for the experiment, a strong tip−surface interaction was observed. This meant that fibrils and other structures adhered to the tip during imaging. In the cases where it was possible to obtain images in situ, it was found that there were no discernible differences in the topographical information obtained when compared to the images of the dried samples.

Figures 5−7 show AFM images taken of the two protein-coated lipid surfaces taken over an area of 10 μm × 10 μm. These images were taken after immersion for 20, 60, and 120 min in the denaturing medium, respectively. Images were taken at earlier times, but no fibrils were detected on either of the surfaces. Figure 5 also shows a typical image of the bulk fibrils taken after immersion for 20 min in the denaturing medium. This figure shows that the fibrils formed at both of the surfaces after immersion for 20 min are shorter than those observed in the bulk. The fibrils formed on the DOTAP surface are also shorter ($\approx$0.7 $\pm$ 0.2 μm) than those found on the DOPG surface (typically 1.5 $\pm$ 0.5 μm). The fibrils found on a given surface were observed to have similar lengths. Samples taken from the bulk solution were found to have a broad distribution of lengths and a maximum length of 4 μm. They were found to be larger and more regular in appearance than those found on either of the surfaces.

The inset shown in the center panel of Figure 5 shows a 1.5 μm × 1.5 μm scan of a fibril formed on a DOPG surface. This image shows that there are regions of the fibril that appear to bulge to form a larger less well-defined structure than the fibrils observed in the bulk samples.

Figure 6 shows images of both a DOTAP surface and a DOPG surface after immersion for 60 min in the denaturing medium. The typical length of the observed fibrils was found to be 5.0 $\pm$ 0.2 μm on the DOPG surface and between 1 and 4 μm on the DOTAP surface.

After the fibrils on the surfaces had spent 120 min in the denaturing medium, imaging became difficult because the bulk solution forms a soft clear gel. Although complete removal of this gel from the surfaces was difficult, it was possible to find areas of the sample surface that were not completely coated. This made imaging of isolated fibrils possible. Figure 7 shows images of DOTAP and DOPG surfaces taken after 120 min. The fibrils on the DOTAP surface show much more branching and appear to be linked together in a network of fibrils and large aggregate structures. The structures of the fibrils found on the DOPG surface are much more well defined and show less branching than the DOTAP surface, having morphologies similar to those formed in the bulk solution. The typical lengths of the fibrils observed on the DOPG surface are between 6 and 8 μm. The fibrils on the DOTAP surface are much harder to characterize than the ones on the DOPG surface because of

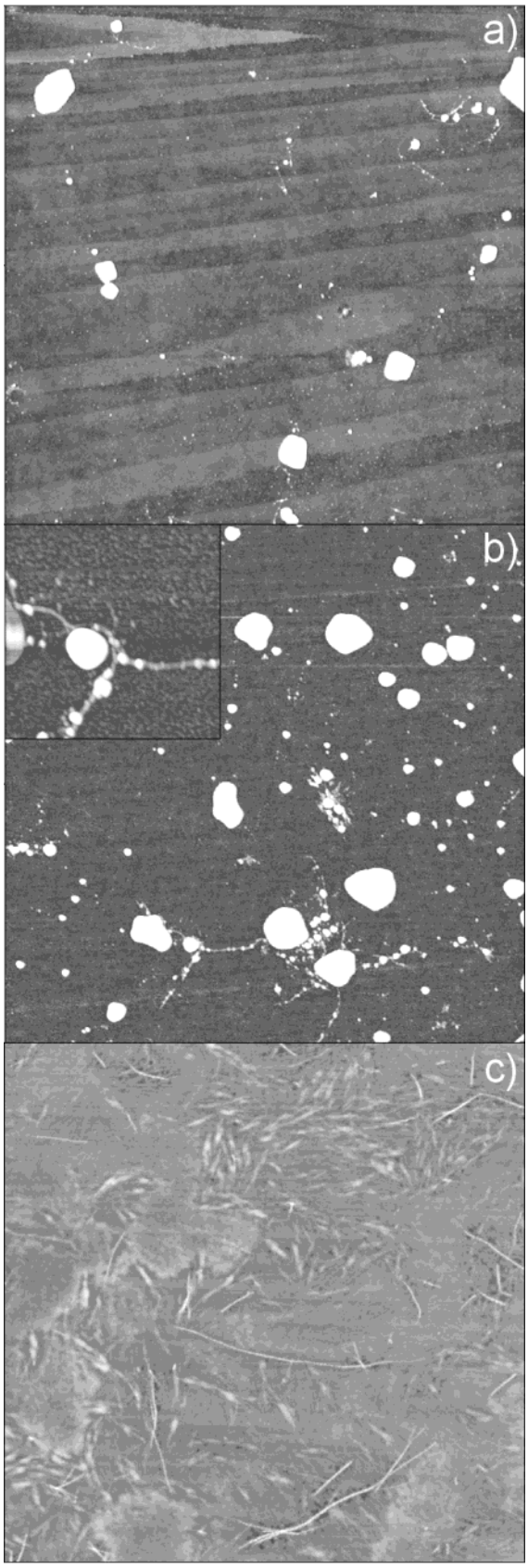

FIGURE 5: AFM images taken over a 10 μm × 10 μm scan area of fibrils formed on the (a) DOTAP and (b) DOPG surfaces and (c) in the bulk solution, after 20 min in denaturing medium (0.025 M HCl and 0.1 M NaCl) at 60 °C. The height scale is 20 nm. The inset (middle panel) shows a 1.5 μm × 1.5 μm scan (20 nm in height) of the DOPG surface.

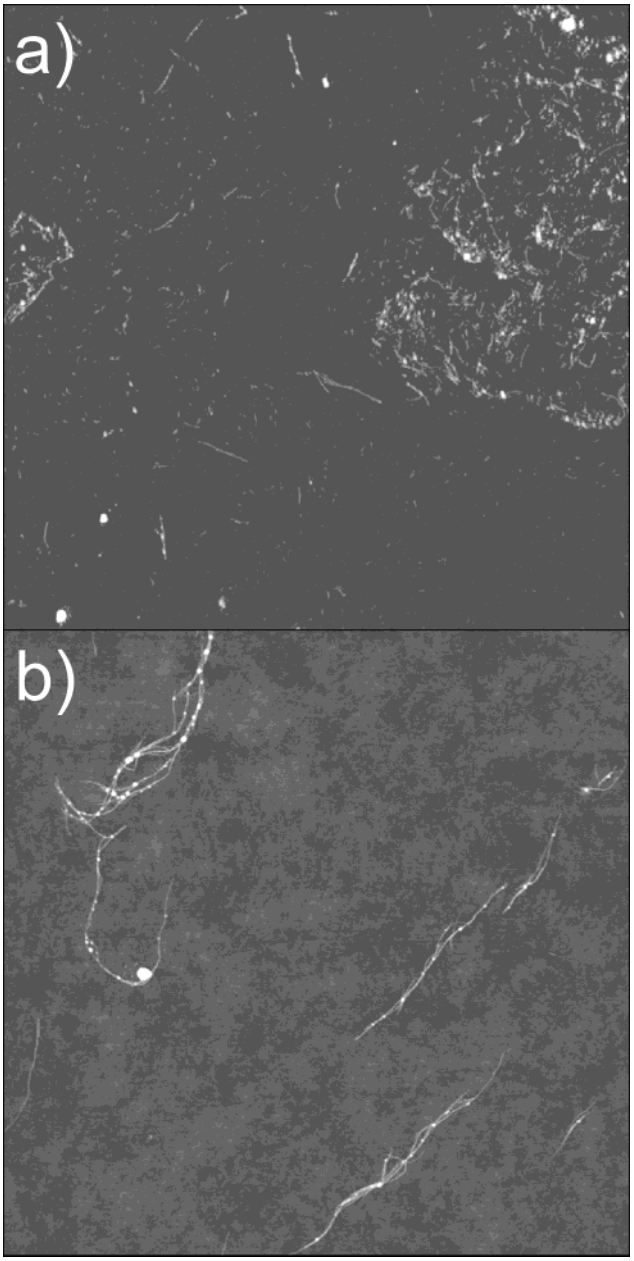

FIGURE 6: AFM images taken over a 10 μm $\times$ 10 μm scan area of fibrils formed on the (a) DOTAP and (b) DOPG surfaces after 60 min in denaturing medium (0.025 M HCl and 0.1 M NaCl) at 60 °C. The height scale is 20 nm.

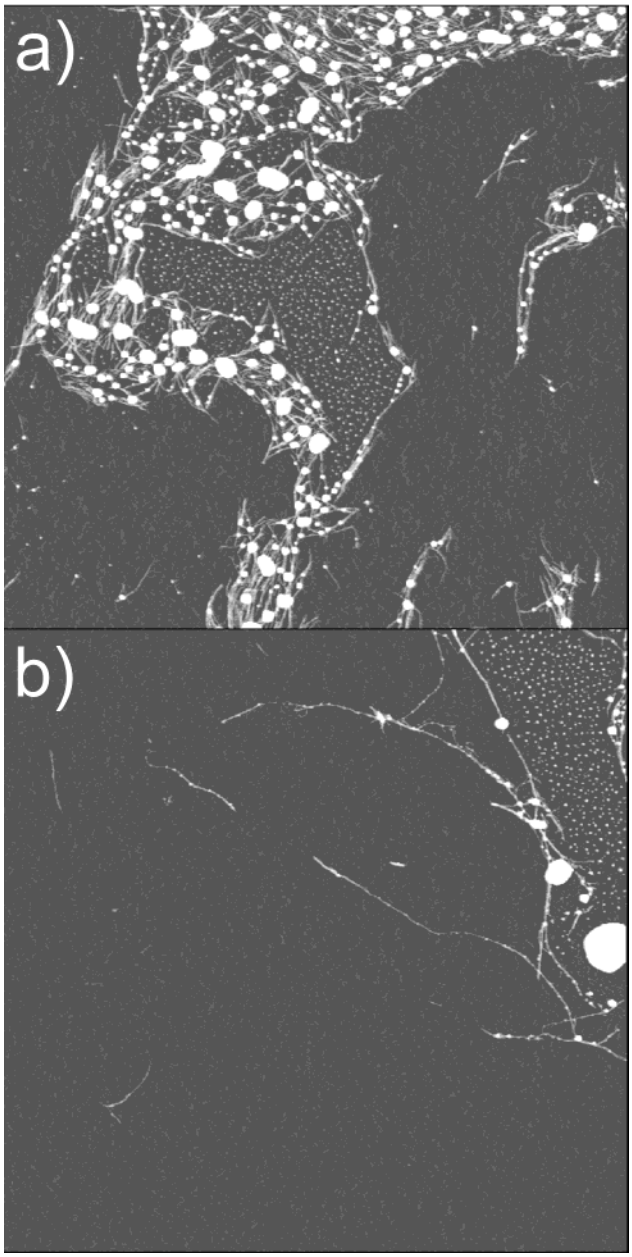

FIGURE 7: AFM images taken over a 10 μm $\times$ 10 μm scan area of fibrils formed on the (a) DOTAP and (b) DOPG surfaces after 120 min in denaturing medium (0.025 M HCl and 0.1 M NaCl) at 60 °C. The height scale is 20 nm.

the presence of the other aggregated structures, but the distance between branching points is typically 1−2 μm.

A direct comparison of the density of fibrils formed at the surfaces with those formed in the bulk is not possible from these images. This is because of the difference in the preparation methods for the samples. It is possible for comparisons to be made between individual fibril dimensions, as well as the morphologies of the fibrils and other aggregates formed.

The root mean square (rms) roughness of the lipid surfaces prior to immersion in the protein solutions was determined using the AFM. This was typically found to 0.45 nm for both of the surfaces studied. These results are consistent with those of Sharp (12) for the roughness of a monolayer of these lipids. The rms roughness of the underlying protein surfaces shown in Figures 5-7 is typically 0.65 nm. The increased roughness of the surface shown in the bottom image of Figure 5 is due to small amounts of recrystallized salt from the denaturing medium. We do not expect this to affect the structure of the observed fibrils because the denaturing medium was removed quickly during the solution drying process (typically a few seconds at room temperature).

The structure of the fibrillar material formed on the lipid surfaces is similar to that observed in the bulk, with only a few exceptions. All of the fibrils imaged have a ribbon-like structure that is 58.1 $\pm$ 2.1 nm wide, and all display a twisted morphology with a period of 61.2 $\pm$ 2.8 nm. The bulk fibrils have a height of 3.9 $\pm$ 0.2 nm at the highest point of the twist and a height of 2.0 $\pm$ 0.1 nm at the lowest point of the twist. The fibrils observed on the surfaces also showed similar height and width profiles except that the surface fibril structures were often found to have unwound on the surface.

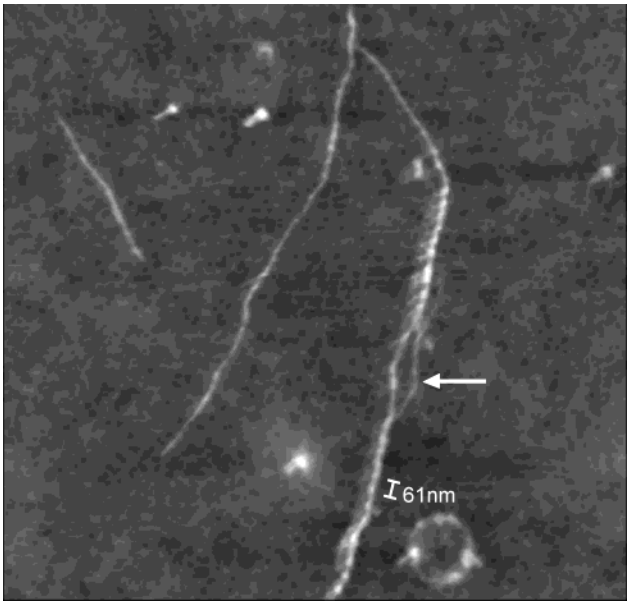

FIGURE 8: AFM image of a fibril on a DOPG surface, taken after 30 min in denaturing medium (0.025 M HCl and 0.1 M NaCl) at 60 °C. The image is taken over an area of 2.5 μm × 2.5 μm (height scale of 10 nm). The arrow marks the place where the ribbon-like structure of the fibril has unwound. The scale bar shows the twist period of the fibrils.

Figure 8 shows a 2.5 μm × 2.5 μm scan of fibrils on a DOPG surface after immersion for 30 min in the denaturing medium. This image shows the twisted structure unfolding to form smaller filaments. A similar effect has also been observed in other systems (*16*). These filaments typically have a height of 2.0 ± 0.1 nm, a value that is consistent with the size of insulin fibrils observed by other authors (*9*, *11*). The fibrils on the lipid surfaces also show more branching than those in the bulk. The unwinding of the fibrils also allows them to rewind with other filaments and produce structures that look similar to the bulk fibrils but that have heights that are integer multiples of 2 nm.

The radius of gyration of the monomeric protein (measured using small-angle X-ray scattering) has been determined to be 1.16 nm at pH 1.6 (*11*). This suggests that the filaments and/or ribbons that are produced are approximately one to two insulin molecules thick and approximately 50 molecules wide. Ribbon-like structures have also been reported in other fibril-forming systems by Goldsbury et al. (*17*). These studies showed that fibrils of amylin displayed a polymorphic structure that arises from the association of individual protofibril filaments. The ribbon structures reported here have widths similar to those reported by Goldsbury et al., but the sizes of the individual filaments that make up the ribbons are slightly larger in the amylin system (typically 5 nm). The electron microscopy images taken in the studies by Goldsbury and co-workers also display a twisted structure with spatial periods similar to those reported for the insulin fibrils studied here (50−100 nm).

Care has to be taken when imaging objects on the 1−2 nm length scale, as convolution of the topographical information with the structure of the AFM tip can be a problem. These problems arise because the nominal radius of curvature of an AFM tip is typically 2 nm and the tip can only effectively image objects that are larger than this size. The fact that the measurements performed on this length scale were out of the plane of the sample makes this less of an issue than it would if the measurements were taken in the plane of the sample. Also, the fact that the fibrils that were imaged were found to have heights that were integer multiples of 2 nm implies that artifacts due to the tip do not play a significant role in determining the out-of-plane fibril dimensions. Of greater concern are the effects of convolution of the in-plane features with the tip structure. The fact that the fibril dimensions reported in this work have been observed in other systems (*17*), using a technique where these convolution effects are not important, is encouraging.

All of the images shown in Figures 6 and 7 show evidence of large aggregate structures. These structures are similar to those reported by Sharp (*12*) that were observed for lysozyme on the same surfaces used here, under what were previously thought to be nondenaturing conditions. The aggregates formed on the DOTAP surface can be up to 500 nm in width and 200 nm in height. Those found on the DOPG surface are on average approximately 300 nm in width and 50−100 nm in height. In general, the aggregates formed on the surface are larger than those observed in the bulk, and although not shown, they can appear in quite dense clusters. The number of these aggregates formed in the bulk is greatly reduced when compared to both of the surfaces.

Role of Surfaces in the Denaturation and Aggregation of Insulin. It is clear from the FTIR and AFM data that the structures formed by insulin molecules under denaturing conditions are influenced by the presence of an interface. So how can we explain this change in behavior and relate the changes in fibril morphology to the structural changes in the protein obtained using the FTIR data?

When a synthetic polymer is confined at a surface, the number of conformations that it can sample is reduced. The resulting entropy changes associated with the polymer are small when compared to the increase in entropy that is caused by displacing small solvent molecules from the surface (*18*). To prevent adsorption of these large molecules, a large repulsive interaction is needed to balance the increase in entropy caused by displacing the small solvent molecules from the interface.

Proteins differ from synthetic polymers in that they have well-defined structures that arise from intramolecular attractions within the protein such as hydrogen bonding (*7*) and disulfide bridges (*7*, *15*). The structures that are formed mean that the protein is restricted to a limited number of conformations in its natural solution state and therefore has a greatly reduced conformational entropy compared to that of synthetic polymers (*14*).

Protein molecules have the potential to increase the number of conformations that they can sample when localized at an interface. This can only happen if the changes in the local conformational free energy landscape (caused by adsorption of the protein) favor a breakdown of the low-entropy structures described above. Under certain conditions, we might expect that proteins can offset some of the loss in translational entropy that occurs due to adsorption at an interface by increasing their conformational entropy. Such an increase in the conformational entropy naturally implies an increased extent of unfolding in the surface-adsorbed protein.

Another possible mechanism for increasing the extent of unfolding is the driving force provided by short-range

enthalpic interactions between the protein and the lipid surface. As suggested by Adams et al. (*6*), unfolding of the protein exposes the more hydrophobic residues at the core of the protein that were previously protected from the aqueous solution.

However, whether the process that leads to the increased rate of unfolding arises because of entropic or enthalpic considerations, the net result is the same, i.e., an increased number of conformations arising form the breakdown of the highly ordered structure of the protein. In fact, the process that leads to the observed rates and extent of unfolding is likely to arise from a combination of both entropic and enthalpic factors.

The data depicted in Figure 3 show an approach to equilibrium for the unfolding of insulin on the repulsive DOTAP surface that is much faster than that observed either on the attractive surface or in the bulk. The presence of a repulsive interaction between the protein molecules and the surface results in an increase in the free energy of adsorption. For adsorption to occur, the protein molecules are required to offset this enthalpy gain in some way. As suggested above, this can be achieved by the protein molecules increasing the entropic component of the free energy of adsorption. An increase in the translational entropy of the adsorbed proteins is forbidden by definition. Therefore, the most likely route by which this can occur is for the protein to further increase the number of conformations that it can sample at this type of interface. This naturally implies a greater rate and equilibrium extent of unfolding in the protein.

An obvious concern regarding this mechanism is that it would result in the breakdown of the well-ordered structure associated with the solution state of the insulin molecules. We might expect that this would introduce energetic barriers to the unfolding process, because of the need to overcome attractive enthalpic interactions within the protein molecules, such as those involved in hydrogen bonding.

Indirect evidence for the breakdown of ordered structures within the molecules can be obtained from the changes in the β-sheet content of the protein. Comparison of Figures 3 and 4 shows that the time scales associated with the changes in β-sheet content are comparable to those for unfolding of the protein molecules. This trend is observed for both of the surfaces studied and in the bulk. Figures 3 and 4 also show a negative correlation between the extent of unfolding and the extent of β-sheet formation per unit volume in the protein, confirming that a greater extent of unfolding results in a more disordered protein structure.

The quantity of protein adsorbed onto both of the surfaces is comparable, although the attractive DOPG surface is observed to have a slightly larger surface excess of insulin than the repulsive DOTAP surface. It is unlikely therefore that the observed difference in β-sheet content of the adsorbed protein is due to changes in packing of the proteins. We might expect this to alter the interpretation of the FTIR experiments if the distribution of molecules relative to the evanescent field is different for the two surfaces. This was confirmed by the fact that no discernible difference can be found between the background of the AFM images shown in Figures 5−8 for the two different protein-covered surfaces, in terms of the thickness or roughness of the adsorbed layers.

The images in Figures 5−8 show that there are a number of differences between the fibrils formed on the surfaces and in the bulk. Comparison of these images with the data shown in Figures 3 and 4 reveals a direct relationship between the extent of unfolding and/or β-sheet content of the adsorbed proteins and the structures that they form during aggregation. This is not surprising. We expect that the number of high-β-sheet content structures (such as fibrils) will be determined by both the extent of unfolding and the amount of β-sheet that the adsorbed protein contains.

The observed increase in the extent of unfolding and reduction in the β-sheet content of the adsorbed proteins can be correlated with a breakdown in the structure of the fibrils that are formed by insulin. The results presented above show that localization of the protein at an interface (either attractive or repulsive with respect to the protein) causes the protein to unfold too much and inhibits the formation of bulk-like fibrils. This is confirmed by the observed breakdown in the internal ordering of the insulin that is manifested as a reduction in the β-sheet content of the proteins.

The reduction in the β-sheet content of the protein is likely to be responsible for the formation of the fibril and/or aggregate structures that are formed at the surfaces. The enhanced unfolding and reduction in the amount of β-sheet in the protein suggest both large changes in the protein conformation and a reduction in the number of structures within the protein that are responsible for aggregation.

CONCLUSIONS

This work considers the effects of confining an insulin molecule at an interface. We use Fourier transform infrared attenuated total reflection (FTIR ATR) spectroscopy to look at how adsorption leads to changes in the unfolding and β-sheet formation kinetics of the protein, when the insulin molecules are placed under denaturing conditions.

The unfolding and β-sheet formation kinetics on lipid-coated surfaces were found to be faster than those reported for the bulk. Insulin adsorbed onto an electrostatically repulsive (DOTAP) surface was shown to have the fastest unfolding kinetics of the two surfaces. The electrostatically attractive (DOPG) surface exhibited slower unfolding kinetics than the repulsive surface, but was shown to have faster unfolding kinetics than the bulk solution protein. A possible explanation was presented in terms of the interplay between enthalpic and entropic processes that control the behavior of protein molecules adsorbed at an interface.

Atomic force microscopy experiments were performed on samples taken both from the bulk solution and from both of the surfaces. This was done so that a comparison of the structures of the aggregates formed in each case could be made. These experiments revealed that the amyloid fibrils formed on both of the surfaces were smaller than those found in the bulk, but that the other types of aggregate were, on average, larger. The reduction in the size and definition of the fibrils formed at the surfaces was attributed to the observed reduction in the content of β-sheet structures within the adsorbed protein molecules.

This work outlines the importance of the role that surfaces play in the denaturation of proteins. For the lipid surfaces that were studied, it shows that adsorption of the protein molecules results in a large amount of unfolding of the protein but a reduction in the level of aggregation in the system.

ACKNOWLEDGMENT

We thank Dr. A. M. Higgins, Dr. R. Staniforth, Dr. S. Adams, and A. Sanders for useful discussions during the course of this work.

REFERENCES

1. Booth, D. R., Sunde, M., Bellotti, V., Robinson, C. V., Hutchinson, W. L., Fraser, P. E., Hawkins, P. N., Dobson, C. M., Radford, S. E., Blake, C. C. F., and Pepys, M. B. (1997) *Nature 385*, 787−793.
2. Terzi, E., Hölzemann, G., and Seelig, J. (1997) *Biochemistry 36*, 14845−14852.
3. Matsuzaki, K., and Horikiri, C. (1999) *Biochemistry 38*, 4137−4142.
4. Sluzky, V., Tamada, J. A., Klibanov, A. M., and Langer, R. (1991) *Proc. Natl. Acad. Sci. U.S.A. 88*, 9377−9381.
5. Ball, A., and Jones, R. A. L. (1995) *Langmuir 11*, 3542−3549.
6. Adams, S., Higgins, A. M., and Jones, R. A. L. (2002) *Langmuir 18*, 4854−4861.
7. Bouchard, M., Zurdo, J., Nettleton, E. J., Dobson, C. M., and Robinson, C. V. (2000) *Protein Sci.*, *9*, 1960−1967.
8. Sipe, J. D., and Cohen, A. S. (2000) *J. Struct. Biol. 130*, 88−98.
9. Burke, M. J., and Rougvie, M. A. (1972) *Biochemistry 11* (13), 2435−2439.
10. Clark, A. H., Saunderson, D. H. P., and Suggett, A. (1981) *Int. J. Pept. Protein Res. 17*, 353−364.
11. Nielsen, L., Khurana, R., Coats, A., Frokjaer, S., Brange, J., Vyas, S., Uversky, V. N., and Fink, A. L. (2001) *Biochemistry 40*, 6036−6046.
12. Sharp, J. S. (2001) Ph.D. Thesis, University of Sheffield, Sheffield, England.
13. Buijs, J., Costa Vera, C., Ayala, E., Steensma, E., Hakansson, P., and Oscarsson, S. (1999) *Anal. Chem. 71*, 3219−3225.
14. Fersht, A. (1999) *Structure and Mechanism in Protein Science*, Freeman, New York.
15. Bryant, C., Spencer, D. B., Miller, A., Bakaysa, D. L., McCune, K. S., Maple, S. R., Pekar, A. H., and Brems, D. N. (1993) *Biochemistry 32*, 8075−8082.
16. Goldsbury, C., Kistler, J., Aebi, U., Arvinte, T., and Cooper, G. J. S. (1999) *J. Mol. Biol. 285*, 33−39.
17. Goldsbury, C., Cooper, G. J. S., Goldie, K. N., Müller, S. A., Saafi, E. L., Gruijters, W. T. M., Misur, M. P., Engel, A., Aebi, U., and Kisler, J. (1997) *J. Struct. Biol. 119*, 17−27.
18. Jones, R. A. L., and Richards, R. W. (1999) *Polymers at Surfaces and Interfaces*, Cambridge University Press, Cambridge, England.

BI020525Z